



# Investigation of outdoor air pollutant, PM<sub>2.5</sub> affecting the indoor air quality in a high-rise building

Nuodi Fu<sup>1,2</sup>, Moon Keun Kim<sup>3</sup> , Bing Chen<sup>4</sup>  and Stephen Sharples<sup>2</sup>

## Abstract

This study investigated the impact of outdoor air pollutants on indoor air quality in a high-rise building, considering factors related to the seasons and air infiltration. Further, the impact of atmospheric weather conditions on air infiltration has been analysed in a downtown area of Suzhou, China. The influence of the outdoor air pollution rate on indoor air quality in the office building was investigated based on on-site measurements and computer simulations. Results showed that the impact of outdoor air pollutants on indoor air quality was highest in winter, followed by spring, autumn and summer. Furthermore, multiple factors, which affect the indoor air quality in a high-rise building, have been further investigated in this study, including stack effect, wind effect, infiltration rate, outdoor air pollution rate, seasonal change and air filter efficiency. The significant influence of these factors on the indoor air quality level with floor height variations has been verified. Based on the analysis, a high-efficiency filter is recommended to maintain healthy indoor air quality. Meanwhile, a double-filter system is required if a building is exposed to heavily polluted outdoor air considering the most substantial impact of outdoor air pollutants on indoor air quality in winter. Moreover, a numerical model of steady-state indoor PM<sub>2.5</sub> concentration was established to determine the suitable air filter efficiency and airtightness.

## Keywords

Outdoor air pollution, Indoor air quality, High-rise building, Infiltration, Air filter efficiency, Stack and wind effect

Accepted: 21 July 2021

## Introduction and background

During the last decade, the impact of particulate matter (PM) issues has been highlighted as a top priority in China due to its extreme health harm to human beings. Because of its small size, the fine and ultra-fine PM can readily and deeply access into human lungs, even the bloodstream. Previous research indicated that smaller size particles were the more hazardous to human health, being linked to higher morbidity and mortality.<sup>1–3</sup> Meanwhile, with the rapid urbanization and economic development in many countries, people spend a large share of their time on indoor activities. Concern was also raised by the U.S.A's Environmental Protection Agency (EPA) report that indoor air pollution levels could much more dangerous than the

---

<sup>1</sup>Department of Architecture, Xi'an Jiaotong – Liverpool University, Suzhou, China

<sup>2</sup>School of Architecture, University of Liverpool, Liverpool, UK  
<sup>3</sup>Department of Civil Engineering and Energy Technology, Oslo Metropolitan University, Oslo, Norway

<sup>4</sup>Department of Urban Planning and Design, Xi'an Jiaotong – Liverpool University, Suzhou, China

### Corresponding author:

Moon Keun Kim, Department of Civil Engineering and Energy Technology, Oslo Metropolitan University P.O. Box 4, St. Olavs plass NO-0130 Oslo Norway Tel.: +47 67 23 65 57  
Email: Moon.Kim@oslomet.no Moon.Kim@oslomet.no

outdoor levels.<sup>4</sup> For example, the indoor PM<sub>2.5</sub> (particles that have diameter less than 2.5 micrometres) level in an office building could be three times higher than the value recommended by the U.S.A' National Ambient Air Quality Standard (NAAQS).<sup>5</sup> Providing a healthy indoor environment in office buildings has a crucial positive impact on employees' health and working efficiency. According to statistics,<sup>6</sup> the number of high-rise buildings has increased dramatically, with around 86% of office buildings now being over 100 m high. Hence, a 100-m tall office building was selected as the objective building in this study.

Airborne particles in buildings come from the outdoors through the building envelope with infiltrating air or the ventilation system's leakages.<sup>7-12</sup> Two existing strategies have been widely used to control IAQ in buildings: installing a high-efficiency air filter system<sup>10,13-15</sup> and increasing the ventilation rate.<sup>10,13,16-20</sup> In mechanically ventilated buildings, the outdoor particles, which infiltrate through gaps in the building's envelope with the infiltration air, could directly impact IAQ. Furthermore, air infiltration could increase the building's heating load by 25% to 30%.<sup>21,22</sup> Infiltration could negatively affect indoor thermal comfort, ventilation system efficiency and acoustic insulation performance.<sup>22,23</sup> Hence, infiltration air is undesired if the outdoor air is contaminated. It is crucial to predict the infiltration rate and to help designers develop a more appropriate design strategy to improve the IAQ.

Infiltration is the unplanned flow of outdoor air into the internal space through cracks in the building and leakage points in the building envelope.<sup>24</sup> The stack effect and the wind effect are the two main mechanisms for developing pressure differences between inside and outside, and both contribute to the air exchange through cracks and cavities in the building. Based on the ASHRAE Handbook of Fundamental,<sup>24</sup> the wind-induced pressure difference increases with height. Meanwhile, the stack-induced pressure differences vary with the difference in height between inlet and outlet openings affected by the location of the neutral pressure level (NPL).<sup>25</sup> Hence, the total pressure difference on the windward facade varies with the building height, which results in air infiltration rates varying between each floor of a building which, in turn, means that the different air infiltration rates will cause IAQ conditions to differ on each floor. However, there is little research about how the air infiltration rate's vertical variation affects each floor's indoor pollutants' concentration. The understanding of this effect could help maintain a good IAQ while simultaneously saving energy.

In addition, many studies have shown that fine and ultra-fine particles have a higher possibility of entering the indoor environment through the ventilation system than coarse particles due to their smaller size, and also

it is hard to capture them using a conventional air filter.<sup>2,26</sup> Small size particles are also easier to infiltrate and penetrate buildings than coarse particles.<sup>27</sup> Hence, the particles are smaller than of 2.5  $\mu\text{m}$ , as PM<sub>2.5</sub>, were considered in this research. Compared to the ambient PM standard, the indoor PM control standard lacks development since only a few countries have established indoor PM control standards. The existing recommended concentration limit for indoor PM<sub>2.5</sub> concentration is mainly aimed at industrial environments.<sup>28</sup> Therefore, the World Health Organization (WHO) Air Quality IT-1 level<sup>29</sup> of 35  $\mu\text{g}/\text{m}^3$  for PM<sub>2.5</sub> was chosen to evaluate the indoor PM<sub>2.5</sub> concentrations in this study.

The objective building for this study was in Suzhou, which is a major city in the southeast of Jiangsu Province, China. The city is a typical industrialized city developed over recent decades. Based on a statistical analysis of historical hourly weather data between 1 January 1980 and 31 December 2018,<sup>30</sup> the temperature typically varied from 0°C to 33°C in Suzhou. The coldest day of the year was 19 January with an average outdoor air dry-bulb temperature of 4°C, while the average ambient air temperature reached up to 30°C on the hottest day of the year (28 July). Accordingly, the climate of Suzhou is hot in summer and cold in winter.

During the last five years, airborne particle pollution has been a persistent problem in Suzhou due to its large manufacturing sector. Since natural ventilation is rarely used, mechanical ventilation systems are necessary for office buildings in Suzhou. Moreover, the wind speed varies slightly between seasons in Suzhou, and the wind direction in Suzhou changes throughout the year. According to weather statistics,<sup>30</sup> the windiest day of the year is 2 May with an average speed of 4.4 m/s. The wind speed was measured at 10 m above the ground. While on the calmest day of the year (23 October), the average wind speed was 3.8 m/s. During spring and autumn, there is a relatively low air temperature difference between indoors and outdoors. The relatively high wind speed can impact on air infiltration in high-rise buildings.

In summary, this study aims to investigate how outdoor air pollutants affect indoor air quality through the leakage in the building envelope in a high-rise mechanically ventilated building. This study's results contribute to a better understanding of the role of air infiltration requirements for controlling the negative impact of airborne particles on human health for buildings in polluted cities. To this end, three research questions have been defined:

1. How do ambient meteorological conditions affect the air infiltration rates?

2. How do the air infiltration rates affect the IAQ in a high-rise mechanically ventilated building?
3. How does the air filter efficiency affect the ingress of outdoor airborne particle concentrations?

## Methodology

To investigate the influence of weather conditions on infiltrating air, Suzhou's daily average meteorological conditions in 2018 were collected from the China Meteorological Bureau database to estimate the daily and seasonal variation of air infiltration rate on each building floor. Furthermore, to answer the second research question, field measurements and numerical simulations were undertaken to predict the IAQ on each floor of a building under different circumstances, including various outdoor air conditions and building locations. Additionally, according to the IAQ simulation results on each floor, different efficiency air filters were applied to investigate the effects of filter efficiency in controlling the indoor PM concentrations.

The methodologies for analysing the impact of increasing outdoor pollution level on IAQ in a high-rise mechanically ventilated building can be subdivided into four steps: (1) Estimate the daily and seasonal variation of the air infiltration rate based on collected data; (2) Perform on-site vertical profile measurements of outdoor air pollutants up the height of the building; (3) Develop numerical simulations based on collected data to predict indoor PM<sub>2.5</sub> level on each floor of the building by using power-law equations; (4) Compare the indoor PM<sub>2.5</sub> levels for different air filter efficiencies.

### Designed office building

As a case study, a hypothetical office building was modelled. The footprint plan area of the building was 259.64 m<sup>2</sup>, which was around 16.11 m (W) × 16.11 m (L), and the floor height was chosen as a typical value of 3.33 m. Thus, the volume of each floor was 865.60 m<sup>3</sup>. The building was 30 storeys high (about 100 m in total). The building faced south and was located in the old downtown of Suzhou, and the building has a maximum of 28 occupants on each floor. Furthermore, in this study, the default ventilation rate was assumed to be 30.6 m<sup>3</sup>/h per person,<sup>31</sup> which equated to approximately 1.0 ACH in each breathing zone.

### Instrumentation

A TSI Model 8534 DustTrak Aerosol Monitor (TSI incorporated USA) was used to measure PM<sub>2.5</sub> concentrations. As a handheld instrument, the 90° light scattering technique, in which the amount of scattered light is proportional to the volume concentration of an aerosol, was applied to estimate concentration values. The

mass resolution of the DustTrak is 1 μg/m<sup>3</sup> or ±0.1% of the reading, while the detection range is from 0.1 to 15 μm approximately. This instrument has been used to measure the atmospheric particles in several widely accepted papers.<sup>32,33</sup> The instrument was calibrated using Arizona Test Dust by the manufacturer to relate light scattering intensity to aerosol mass concentrations and be recalibrated at the experiment site before every measurement.

### Test sites and experimental description

Due to the experiment site's limitation, a case study was conducted to investigate the outdoor particles' vertical profile. The measured data were then compared with published data which were measured in a city close to Suzhou, to see whether those data could be applied in this case study. The selected building, which will remain anonymous, was approximately 12 storeys tall (~63 m). The test building was located in a relatively open area surrounded by a pedestrian road and a vehicle road. Time-resolved measurements were conducted during two periods in different seasons: spring (9:00 am–11:00 am, 27 March–3 April 2019), summer (9:00 am–11:00 am, 20 May–27 May 2019), autumn (9:00 am–11:00 am, 15 October–22 October 2019) and winter (9:00 am–11:00 am, 26 November–02 December 2019).

Samples were collected on the first floor (1.2 m) and 12<sup>th</sup> floor (62.6 m). The calibrated instrument was placed outside of each floor's balcony that faced a square, approximately 1.2 m above each floor level and 1 m away from the building façade. One researcher with an instrument was deployed on each sampling site in this study, ensuring the same logging interval (10 s) was used. The locations of building A and building B in the experimental site are illustrated in Figure 1.

### Weather characteristics

Suzhou is located in the Yangtze River Delta's central part in China's east (31°18'N 120°36'E), and it borders Shanghai. The city is situated in the subtropical zone, which indicates that it experiences a warm and moist monsoon maritime climate. The meteorological conditions of Suzhou in 2018 were used to analyse the seasonal variation of the impact of outdoor air pollutants on indoor air quality. The daily average outdoor air dry-bulb temperature and wind speed from 1 January 2018 to 31 December 2018 are shown in Figures 2 and 3. From Figures 2 and 3, the outdoor air temperature of Suzhou in 2018 varied from 0°C to 32°C. Furthermore, ambient wind speed ranged between 0.3 m/s and 8.3 m/s. Since the outdoor temperature is slightly affected by altitude decreasing by around 0.6°C per 100 m increase of altitude,<sup>36</sup> the outdoor

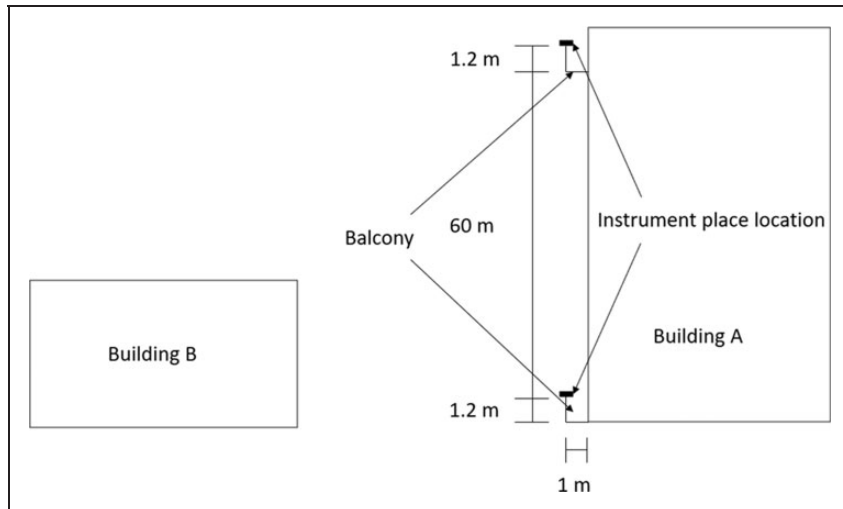


**Figure 1.** The detailed information of the experiment site.

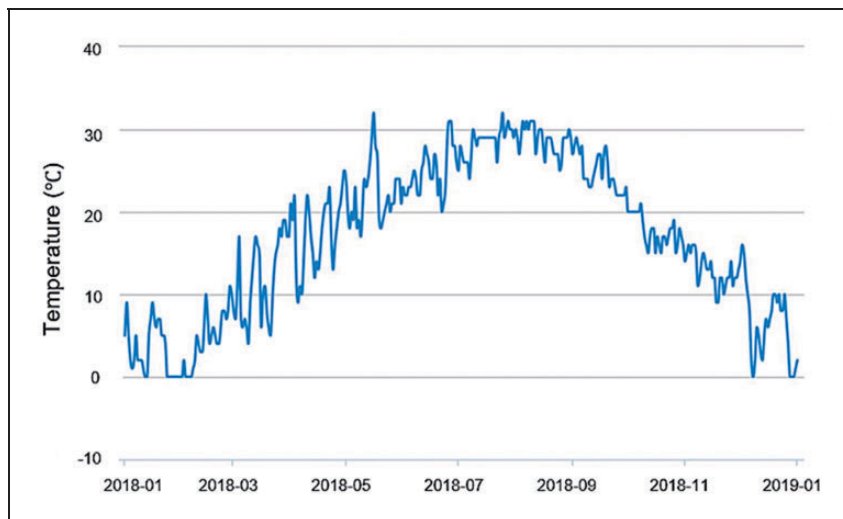


**Figure 2.** Suzhou daily average outdoor dry-bulb air temperature from 1 January 2018 to 31 December 2018.<sup>34</sup>

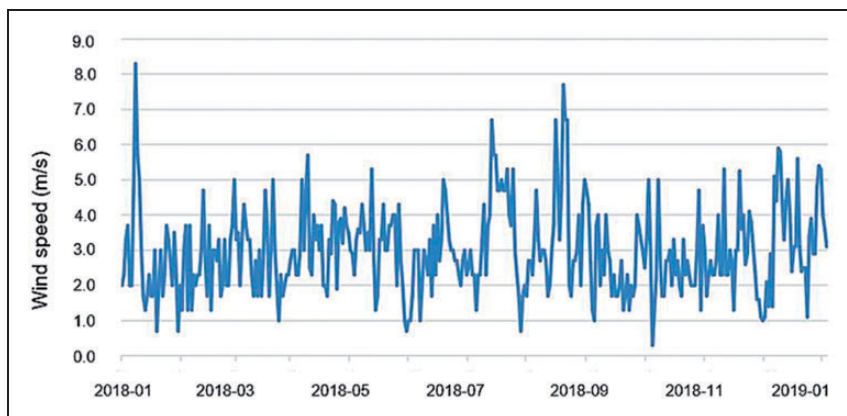


**Figure 3.** Suzhou daily average wind speed from 1 January 2018 to 31 December 2018.<sup>35</sup>

air temperature, in this case, was kept constant with up the building's height. For the assessment of indoor thermal comfort, the ASHRAE Standard 55–2010 was used. This meant that the target indoor air temperature was set at 24°C in the cooling season, the target room temperature was set at 20°C in the heating season and the target indoor air temperature was set at 22°C in both the spring and autumn seasons.<sup>37</sup>

### Analysis of indoor PM concentration

Over time, indoor PM concentration levels can be remodelled as a function that mainly depends on source terms and loss terms. Assume that the particle concentration in the room is uniform,<sup>38</sup> equation (1) represents the dynamic solution of the mass balance equation that describes the indoor concentration.<sup>10,39–41</sup>

$$\begin{aligned} \text{PM}_{in,t_k} = & \text{PM}_{in,t_{k-1}} \times e^{-L(t_k-t_{k-1})} \\ & + \left( \frac{S}{L} - \frac{S}{L} \times e^{-L(t_k-t_{k-1})} \right) \end{aligned} \quad (1)$$

where  $\text{PM}_{in,t_k}$  is the concentration of the indoor PM concentration at time  $k$  in  $\mu\text{g}/\text{m}^3$ ,  $S$  is the source term,  $L$  is the loss term and  $t_k$  is the ventilation system's operation time. This study assumed that there were no indoor particle emission sources, which indicates that the indoor PM level will be equal to or lower than the outdoor levels at steady-state.<sup>42</sup> Thus, the indoor  $\text{PM}_{2.5}$  concentration was defined as equal to the ambient level at the beginning of the simulation. For the source term, the origin of  $\text{PM}_{2.5}$  in the indoor environment was the outdoor air coming through the ventilation system or penetrating through building cracks and wall cavities in a mechanically ventilated building.<sup>9,13,43,44</sup> To simplify the simulation, the air in the ventilation system was assumed not to be recirculated, and there were no indoor PM emission sources. Moreover, compared to the deposition rate, the particle resuspension rate induced by indoor human activities was weak enough to be neglected,<sup>45</sup> so that the source term can be expressed by equation (2)

$$S = C_{out} \times \lambda_v \times (1 - \eta_{AHU}) + C_{out} \times p \times \lambda_i \quad (2)$$

where  $C_{out}$  is the outdoor particle concentration in  $\mu\text{g}/\text{m}^3$ ,  $\lambda_v$  is air change rate attributed to ventilation,  $\eta_{AHU}$  is the air-handling unit filter efficiency,  $p$  is the penetration rate of particles, which was set to 0.95 for  $\text{PM}_{2.5}$  and  $\lambda_i$  is the air change rates attributed to the infiltration rate. In this study, several air filters with different efficiencies for removing the  $\text{PM}_{2.5}$  were considered.<sup>46,47</sup> Furthermore, the loss terms contain the air

pollutant removal mechanisms by ventilation and deposition onto indoor surfaces. Hence, the loss term can be expressed by equation (3)

$$L = \lambda_v + \lambda_i + \beta \quad (3)$$

where  $\beta$  is the deposition rate, which is  $0.5\text{h}^{-1}$  for  $\text{PM}_{2.5}$ .<sup>10,48</sup>

**Estimation of infiltration rate.** Both stack and wind effects are required to determine the pressure difference between the indoors and outdoors to estimate of the air infiltration rate in a building. In addition, the infiltration rate is also affected by the type of air pollutants, building surface material and crack geometry.<sup>27,43,49,50</sup> Because this paper aimed to investigate the impact of outdoor air pollutants on the IAQ in a high-rise mechanically ventilated building, several presumptions were made:

1. The building that was used in the case study is rectangular.
2. Leakage was uniformly distributed on the south facade of the building, and there was no leakage in the other three facades.
3. Crack geometry was uniform. It means that it is an idealized rectangular straight crack with a fixed dimension throughout the leakage path, that the inner surface of the crack is smooth, and that the airflow is the stable laminar flow through the crack. Further, the width of the crack is greater than that height. This means that the airflow can be reasonably thought of as a two-dimensional model.
4. Indoor air temperature was assumed to be uniform.
5. Average values of the wind pressure coefficients were used in this study.
6. Particle size distribution was assumed to be uniform.
7. Fan operation was independent of any wind-induced or stack-induced pressure differences imposed across it.

Based on the ASHRAE Handbook,<sup>24</sup> the local wind pressure on buildings can be determined by equation (4)

$$p_w = 0.5 \times C_p \times \rho_o \times U_H^2 \quad (4)$$

where  $p_w$  is the local wind pressure on the building surface in Pascal (Pa),  $C_p$  is the local wind coefficient, which is a dimensionless value and can be determined with the surface-average wall pressure coefficient for high-rise building curve,<sup>24</sup>  $\rho_o$  is the outdoor air density in  $\text{kg}/\text{m}^3$ , and  $U_H$  is the approach wind speed at

upwind wall height  $H$  in m/s. This wind speed can be described by equation (5)

$$U_H = U_{met} \times \left( \frac{\delta_{met}}{H_{met}} \right)^{a_{met}} \times \left( \frac{H}{\delta} \right)^a \quad (5)$$

where  $U_{met}$  is the reference wind speed measured at the meteorological station in m/s,  $\delta$  and  $\delta_{met}$  are the atmospheric boundary layer thicknesses for the local building and meteorological station, respectively,  $a$  and  $a_{met}$  are the exponent for the local building terrain and meteorological station terrain, respectively,  $H_{met}$  is the height at which the reference wind speed has been measured, typically 10 m above the ground level, and  $H$  is the wind speed that occurs at a specific height, which is defined as the mid-point on each floor to represent the specific wind speed at that floor in this study. Then the wind pressure on the building facade can be expressed with the coefficient  $C_{p(in-out)}$  and based on the atmospheric boundary layer parameters provided by the ASHRAE handbook.<sup>24</sup> For the building located in the urban area, the wind pressure is presented by equation (6)

$$\Delta p_w = 0.5 \times (C_p - C_{pi}) \times \rho_o \times \left( U_{met} \times 1.586 \times \left( \frac{H}{460} \right)^{0.33} \right)^2 \quad (6)$$

where  $\Delta P_w$  is the wind-induced difference between indoor and outdoor pressure, and  $C_{pi}$  is the internal wind pressure coefficient, which is around  $-0.2$  for a building in which the air leakage sites are distributed uniformly in all the walls.<sup>51</sup> For tall buildings, the stack-induced pressure difference for a horizontal leak at any vertical location in the building can be characterized by a sufficient stack height and neutral pressure level (NPL), which is expressed by equation (7)<sup>24</sup>

$$\Delta p_s = C_d \times \rho_o \times \left( \frac{T_i - T_o}{T_i} \right) \times g \times (H_{NPL} - H) \quad (7)$$

where  $\Delta P_s$  is the stack-induced difference between indoor and outdoor pressure in Pa,  $C_d$  is the thermal drift coefficient,  $\rho_o$  is the outdoor air density in  $\text{kg/m}^3$ ,  $g$  is the gravitational acceleration constant ( $9.81 \text{ m/s}^2$ ),  $H_{NPL}$  is the height of the NPL above the reference plane in m and  $H$  is the height above the reference plane in m. The variable  $C_d$  is a correction factor to describe the pressure difference between each floor caused by resistances (e.g. doors), and its value for office buildings varied from 0.63 to 0.82.<sup>51</sup> In this study, an average value of  $C_d = 0.725$  was applied, and the stack pressure on each floor's mid-point was used to represent the average stack pressure on that floor.<sup>51</sup>

In theory, the NPL is precisely at the mid-height of a building if the building's cracks and other openings are uniformly distributed vertically.<sup>24,51</sup> However, many factors, including the mechanical supply and exhaust system, affected the indoor air pressure level and contributed to the NPL location variation.<sup>25,44,45,52,53</sup> Hence, this study defined the NPL at 30%, 50% and 70% of the total building height to investigate the stack-induced pressure difference between the inside and outside of the building.<sup>24</sup> Then the total pressure difference can be calculated by equation (8)

$$\Delta p = \Delta p_w + \Delta p_s \quad (8)$$

After determining the total pressure difference between indoors and outdoors, the air infiltration rate could be determined by equation (9)<sup>24</sup>

$$\lambda_i = \left( \frac{3600}{V} \right) \times c \times (\Delta p)^n \quad (9)$$

where  $V$  is the breathing zone volume ( $\text{m}^3$ ),  $n$  is the exponent, as a dimensionless value of 0.65 (ASHRAE, 2017).<sup>24</sup> The flow coefficient  $c$  is in the unit of  $\text{m}^3/(\text{s} \cdot (\text{Pa})^n)$ , which is described by equation (10)<sup>24</sup> as

$$Q = c \times (\Delta P)^n \quad (10)$$

where  $Q$  is the airflow through the opening in  $\text{m}^3/\text{s}$ . Based on ASHRAE handbooks (2017),<sup>24</sup> the infiltration rate in the office building was assumed to be 0.1 ACH at 75 Pa.<sup>24</sup> Accordingly, the value of the flow coefficient,  $1.453 \times 10^{-3} \text{ m}^3/(\text{s} \cdot (\text{Pa})^{0.65})$ , can be substituted into equation (11) as

$$\lambda_i = 0.006044 \times (\Delta p)^{0.65} \quad (11)$$

## Results and discussion

### Prediction of the pressure difference between indoors and outdoors

Based on the collected data, all calculations were carried out to change the pressure difference between both sides of the building's south facade in a year.

*The impact of meteorological conditions on the pressure difference between indoors and outdoors.* For a typical year, Suzhou's daily averaged outdoor air temperature varies between  $0^\circ\text{C}$  (273 K) and  $32^\circ\text{C}$  (305 K). The temperature difference between

the inside and outside ( $D_T = T_i - T_o$ ) ranges from  $-8\text{ K}$  to  $20\text{ K}$  to compare with the chosen indoor air temperature. The impact of outdoor air temperature on stack-induced pressure difference is displayed in Figure 4, which shows that the stack-induced pressure difference was positively correlated with the  $D_T$ . Furthermore, if the indoor air temperature is higher than outdoor, such as in winter, the air tended to be exfiltrated into the indoor environment from outdoors on lower floors, whereas it tends to be infiltrated on upper floors. Conversely, airflow behaviours performed oppositely when indoors' temperature was lower than outdoors, such as in summer. The outdoor air is infiltrated into an indoor environment on lower floors, and such air is exfiltrated on the upper floors.<sup>44</sup>

Based on the simulation results, when the difference between inside and outside temperature increased by  $5\text{ K}$ , the stack-induced pressure difference on the building facade doubled. However, the increasing proportion of the pressure difference decreased near the transition point (where the stack-induced pressure difference equals 0). This means that the stack-induced pressure difference was linearly proportional to the building height.

From reference, the ambient wind speed in 2018 varied from  $0.3\text{ m/s}$  to  $8.3\text{ m/s}$ . Based on such data sources, simulations were carried out to investigate the impact of ambient wind speed on wind-induced

pressure difference, and the results are shown in Figure 5. Figure 5 indicates that the wind-induced pressure difference was also increased with an increase in the outdoor wind velocity, while the increased margin of the pressure difference was increased along with the building height. More specifically, the pressure difference was increased from  $0.02\text{ Pa}$  to  $1.98\text{ Pa}$  on the ground floor if the ambient wind velocity rose from  $1\text{ m/s}$  to  $8\text{ m/s}$ , while on the top floor, it rose from  $0.32\text{ Pa}$  to  $29.20\text{ Pa}$ . A non-linear correlation between the wind-induced pressure and the building height can be determined from Figures 4 and 5.

Since the wind speed does not affect the variation trend of pressure difference in the vertical direction, the annual average outdoor wind speed,  $4.1\text{ m/s}$ , was taken as an example to investigate the influence of wind direction on the wind-induced pressure difference. The results are shown in Figure 6. If the wind direction was changed from  $0^\circ$  to  $45^\circ$ , the wind-induced pressure difference was decreased by around  $30\%$  at both the top and ground floors. If the direction changed from  $90^\circ$  to  $180^\circ$ , it caused a  $56.3\%$  decline in the pressure difference. As a special case, the wind-induced pressure difference was reduced to 0 if the direction was around  $70^\circ$ .<sup>24</sup> Overall, the pressure difference between the wind and south facades was proportional to the wind angle with a negative gradient. Furthermore, such a relationship is not affected by the wind speed since the

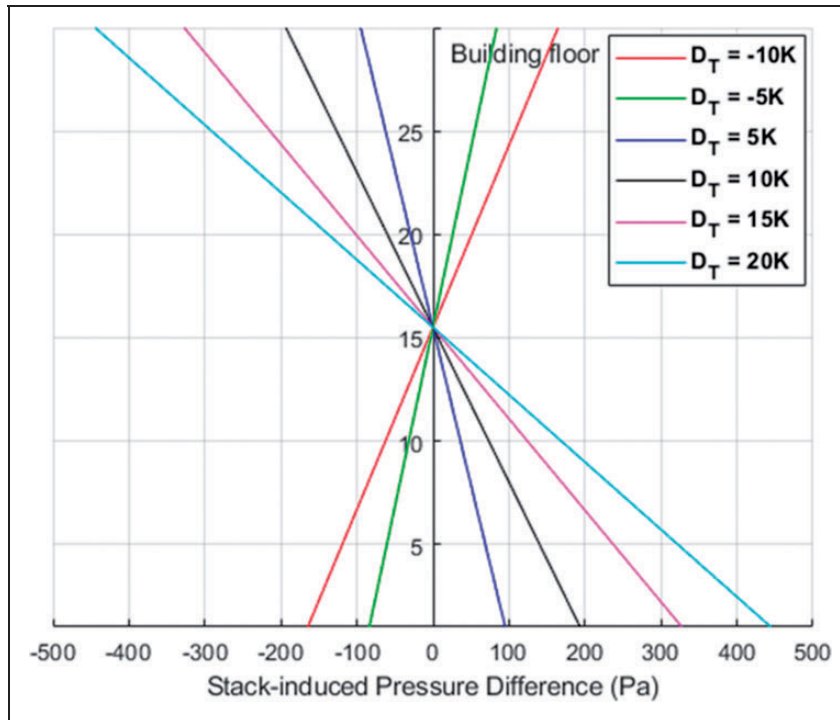


**Figure 4.** The impact of the temperature difference between indoors and outdoors on stack-induced pressure difference when NPL is at 50% of the building height.

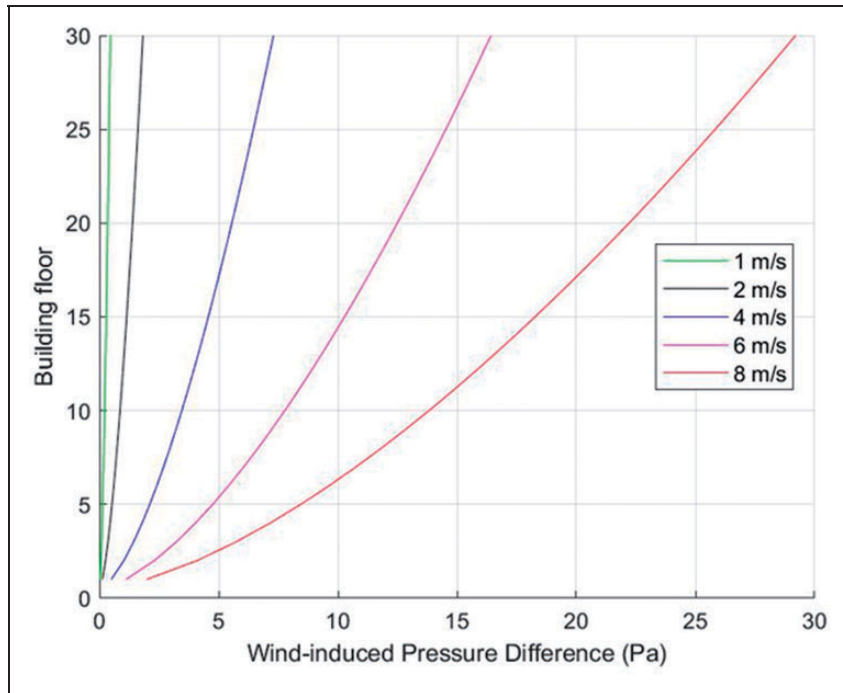


**Figure 5.** The impact of wind speed on wind-induced pressure difference when the wind direction is perpendicular to the building south façade ( $\theta = 0^\circ$ ) when NPL is at 50% of the building height.

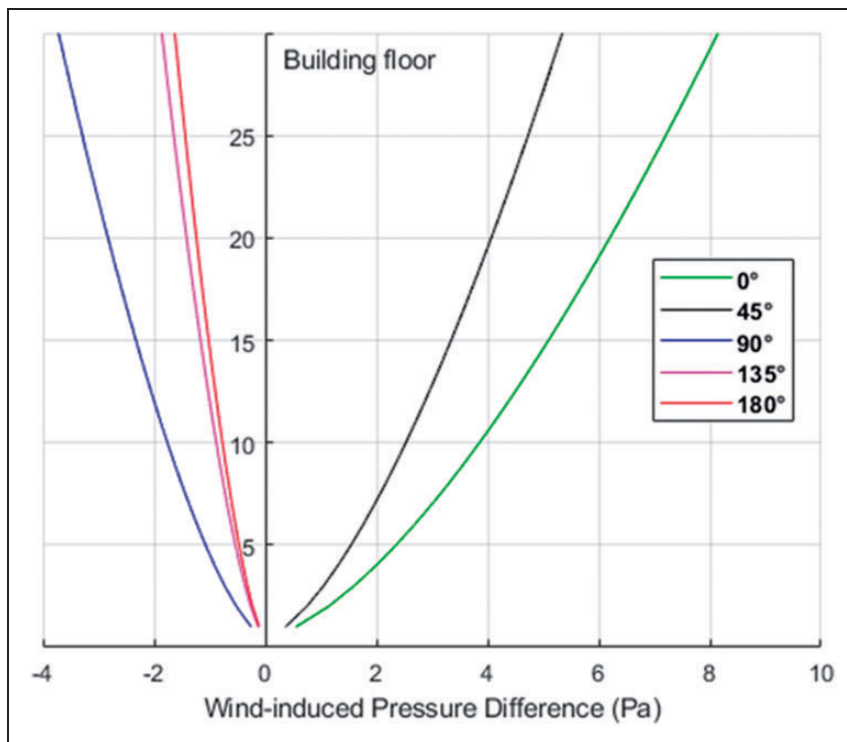


**Figure 6.** The impact of the wind direction on the wind-induced pressure difference when  $U_{\text{met}} = 4.1$  m/s.



gradient stayed constant along with the varying wind speed.

**The impact of the neutral pressure level NPL on the pressure difference between indoors and outdoors.** Figure 7 displays the impact of the NPL on the stack-induced pressure difference when the wind direction was perpendicular to the south facade of the building. These results show that the NPL height had a significant impact on the stack-induced pressure differences on each floor of the building, and it also affected the height of the transition point. When the NPL location was changed from 30% to 70% of the building height, the stack-induced pressure difference fluctuated around 140% on each floor. Based on the results of simulations, the temperature difference did not impact on the fluctuation of the pressure difference on each floor. However, the pressure difference was increased on the lower floor and was decreased on the upper floor if the indoor air temperature was higher. Otherwise, it decayed on the lower floor and rose on the upper floor. Moreover, the transition point occurred at around the 10th floor, 15th floor and 22nd floor if the NPL was set at 30%, 50% and 70% of the building height, respectively.<sup>24</sup>

### Numerical prediction of indoor PM<sub>2.5</sub> concentration

Over the past decade, vertical particle profiles on high-rise office building facades have been focused on by researchers.<sup>33,54–59</sup> Generally, the outdoor airborne particle concentration would decrease with the rise in height. Furthermore, several studies indicate that the outdoor particle concentration shows a stronger apparent decreasing trend with the height in open areas than in urban areas.<sup>33,57</sup> The outdoor particle level's vertical pattern is influenced by many factors, such as atmospheric stability, ambient meteorological conditions and the surrounding environment.<sup>54,58,60,61</sup>

In this study, a case study was conducted to investigate the difference in outdoor PM<sub>2.5</sub> and indoor concentrations between the top floor and the ground floor of a single tall building in Suzhou. The concentration of PM<sub>2.5</sub> was decreased significantly on the top floor throughout the whole year, which is coincident with results determined by previous studies.<sup>33,57,59</sup> On the 12th floor (62.6 m), the averaged PM<sub>2.5</sub> concentration was decreased by 8.4% (3.7%–12.3%), 23.4% (20.5%–34.3%), 17.1% (15.7%–20.9%) and 16.7% (12.2%–23.4%) over four measured periods. In contrast, Liu et al.<sup>33</sup> investigated the vertical profile of PM<sub>2.5</sub> based on a 100 m height office building in an urban area and a mountain in the forest park in Nanjing over four

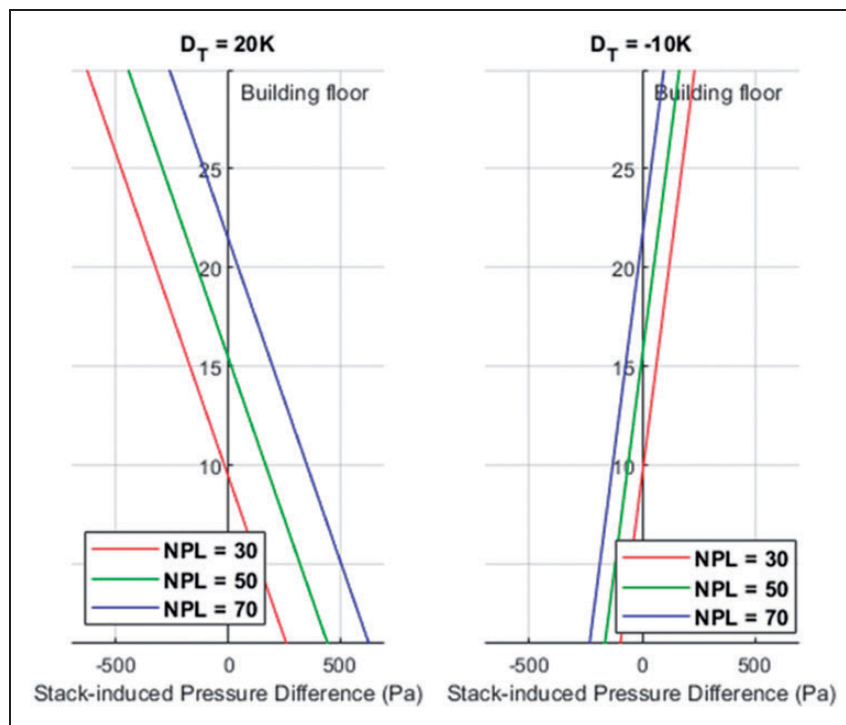


**Figure 7.** The variation law of stack-induced pressure difference along with the building height under different NPL when wind direction is perpendicular to the south façade of the building ( $\theta = 0^\circ$ ).

seasons. They reported that, at 65 m, the averaged  $PM_{2.5}$  concentration decayed 28.1%, 30%, 27% and 15.5% in the forest park, and -0.6% (the  $PM_{2.5}$  level was increased by 0.6% compared with the ground floor), 20%, 16.1% and 10.7% on the urban area over four seasons. The measured result of this study was between the value measured in the urban area and forest park. Thus, the results measured in this study show a good agreement with reference data since the test office building in this study is located in a relatively open space, as well being near a pedestrian road.

Furthermore, Nanjing is very close to Suzhou, and thus the results reported by Liu et al.<sup>33</sup> can be used as a benchmark for investigating the IAQ on each floor of a 100 m tall building. As introduced in the background section, the outdoor  $PM_{2.5}$  concentration was reduced at the top floor in both spring and autumn, while the maximum outdoor  $PM_{2.5}$  level occurred at around 10 m and 25 m in spring and autumn, respectively. Such a phenomenon might be due to the impact of buildings in the surrounding environment, such as the roadside trees, emission sources and surrounding building heights.<sup>33,59,62</sup> However, in both summer and winter, the outdoor  $PM_{2.5}$  level generally decreased with the building height. Based on the results reported by Liu et al.,<sup>33</sup> the seasonal vertical profiles of the outdoor  $PM_{2.5}$  level around the building in this study are presented in Table 1.

**Variation law of IAQ in a high-rise building.** By applying the proposed air infiltration rates on each floor of a building, the hourly variation of indoor  $PM_{2.5}$  concentrations on four selected specific days in 2018 were simulated. The four selected days were 19th January, 2 May, 28 July and 23 October, and the daily average outdoor  $PM_{2.5}$  levels for these four days were

**Table 1.** The seasonal vertical profiles of outdoor  $PM_{2.5}$  level on the south façade of the building.<sup>33</sup>

Height (m)	Spring (%)	Summer (%)	Autumn (%)	Winter (%)
1.65 (1st floor)	0	0	0	0
31.35 (10th floor)	+4.5	-5.5	-6.2	-7.1
51.15 (16th floor)	+3.1	-8.8	-13.6	-9.7
64.35 (20th floor)	+0.6	-20.0	-16.1	-10.7
97.35 (30th floor)	-7.0	-12.9	-18.1	-19.7

**Table 2.** Parameters investigated for indoor  $PM_{2.5}$  concentration.

Particle size	$\eta_a$ (%)	$\lambda_v$ ( $h^{-1}$ )	$\beta$ ( $h^{-1}$ )	p ( $h^{-1}$ )	$C_{out}$ ( $\mu g/m^3$ )
$PM_{2.5}$	32.3 (MERV8)	1	0.5	0.95	47.6, 51.5, 72.1, 199.1

199.1  $\mu g/m^3$ , 47.6  $\mu g/m^3$ , 51.5  $\mu g/m^3$  and 72.1  $\mu g/m^3$ , respectively. All input variables used in the simulation are listed in Table 2.

According to the occupancy diversity factor,<sup>31</sup> an office building's working hours are generally between 06:00 and 21:00. Thus, this study mainly focused on the indoor  $PM_{2.5}$  concentration during working hours, and the results are displayed in Figure 8. Moreover, Figure 9 displays the value range of indoor  $PM_{2.5}$  concentrations on five selected floors of the case study building. Figure 9 shows that the IAQ in the building was the best during summer, followed by spring, autumn and winter. In general, the indoor  $PM_{2.5}$  concentration showed a continuous decrease with the height in both summer and winter. However, a fluctuation was determined during spring and autumn since the outdoor particle level's vertical profile did not steadily decrease with the height. Furthermore, the indoor  $PM_{2.5}$  level showed 7.0%, 12.9%, 18.1% and 19.7% attenuation at the top floor when the season changed from spring to winter. The decreasing trend is the same as the outdoor  $PM_{2.5}$  vertical profile, and the results indicate that outdoor air pollutants have a significant impact on the IAQ.<sup>63</sup>

According to Figure 9, the median line approximately coincides with the 25th percentile and the minimum value line on 19 January. This indicates that the indoor  $PM_{2.5}$  level reached the steady-state quickly due to the significant and stable stack-induced pressure difference between indoors and outdoors. Moreover, the minimum indoor particle levels on the four selected days occurred when the stack-effect was at its maximum, while when the stack-effect was at a minimum, the concentration was maximal. In addition, the range of indoor  $PM_{2.5}$  concentrations was wider in the transition seasons. One reason is that the impact of wind-effect on the air infiltration rate was relatively higher in these two seasons due to the lower stack-effect. The result in this study indicates that the dominant driving force of the infiltrating air in a high-rise building was the stack-effect, which is coincident with the previous research findings.<sup>25,64</sup>

In summary, the IAQ varied evidently per floor of a building, and the outdoor air pollutant level had a significant impact on IAQ in the mechanically ventilated building. The IAQ increased with the building height generally over the year if the outdoor air was contaminated. For the target building in Suzhou, the IAQ was best in the summer, followed by autumn, spring and winter.

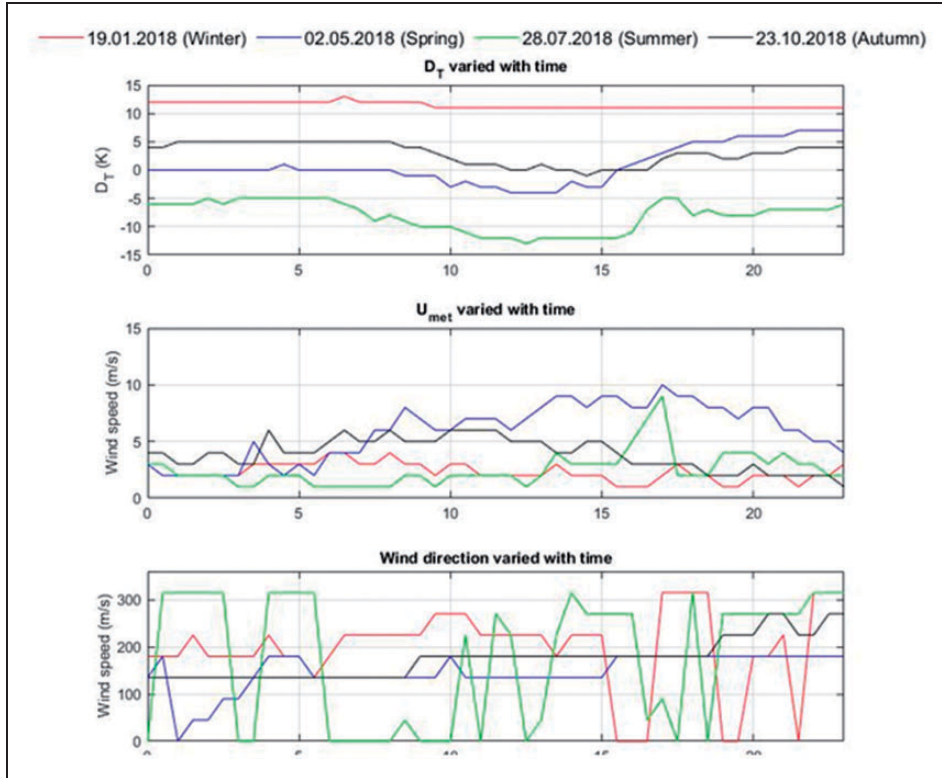


**Figure 8.** The hourly variation of outdoor meteorological conditions on four selected days. ( $D_T$  = indoor air temperature – outdoor air temperature).

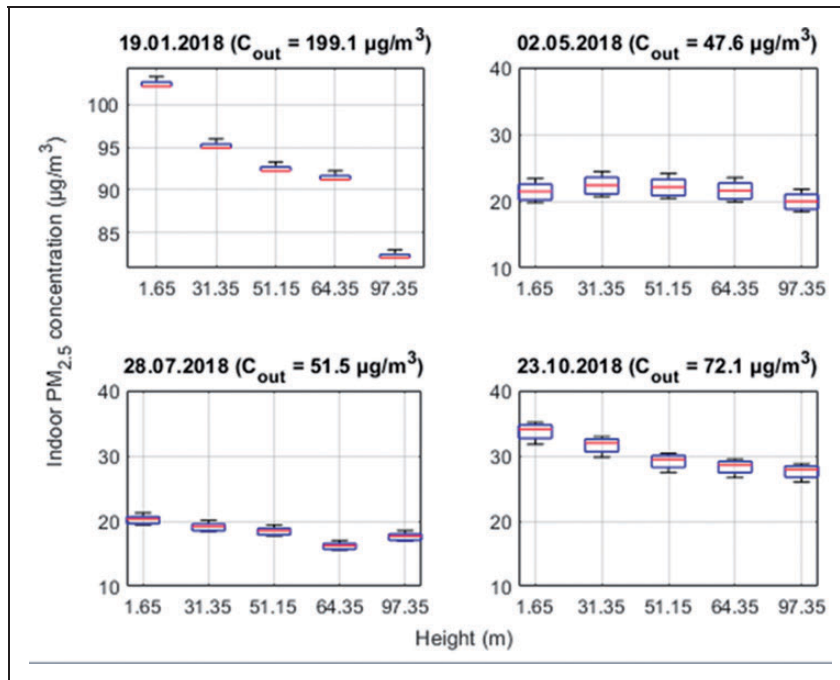


**Figure 9.** The value range of indoor  $\text{PM}_{2.5}$  concentration on five selected floors (in order from left to right is 1st, 10th, 16th, 20th, 30<sup>th</sup> floor) between 6:00 and 21:00 in four seasons when NPL locates at 50% of the building height (the five horizontal lines for each box in order from top to bottom: maximum value, 3rd quartile, median, 1st quartile, minimum value).

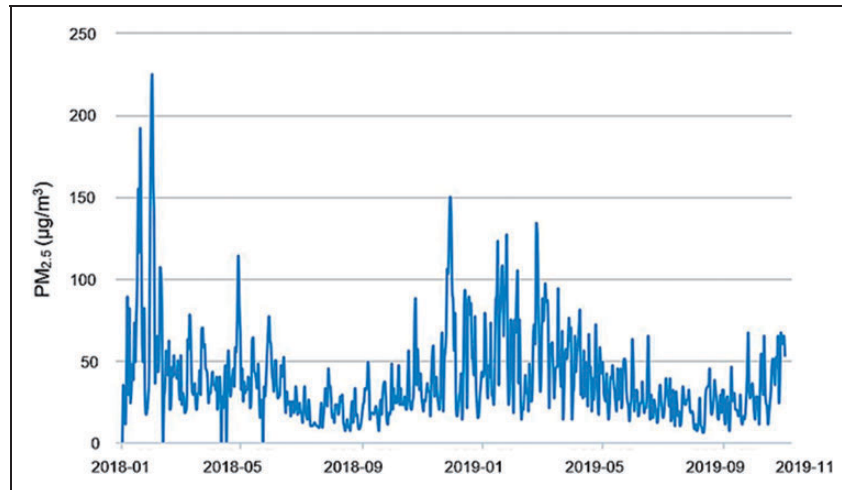


**Figure 10.** The daily average outdoor  $PM_{2.5}$  concentrations in Suzhou between 1 January 2018 and 1 November 2019.<sup>34</sup>

*Impact of neutral pressure level on IAQ.* Figure 10 illustrates that the outdoor air was more heavily contaminated in winter since the  $PM_{2.5}$  level was higher, whereas it was less polluted in both spring and autumn by comparison with summer. In terms of statistics,<sup>34</sup> the daily average outdoor  $PM_{2.5}$  level varied as 15–114  $\mu\text{g}/\text{m}^3$ , 7–52  $\mu\text{g}/\text{m}^3$ , 7–150  $\mu\text{g}/\text{m}^3$ , 11–225  $\mu\text{g}/\text{m}^3$  from spring to winter. The extreme cases have been utilized to investigate the impact of NPL on IAQ on both the ground and top floors of the building. Figure 11 presents the variation of IAQ for the location of the NPL rising from 30% to 70% of the building height. In that situation, the average indoor  $PM_{2.5}$  level was increased by around 0.3%, 2.5%, 6.0% on each floor in spring, autumn and winter, respectively. A different phenomenon was found during summer when it decreased by around 7.5% on each floor of the building. Overall, Figure 11 shows that the location of the NPL was negatively correlated with the indoor particle level if the air temperature is higher indoors. In contrast, it had a positive impact on the IAQ in buildings during summer.

In summary, the NPL had significant effects on IAQ. The results demonstrate that the  $PM_{2.5}$  concentration peaked in winter. Also, from simulations, the number of occupants suffering from  $PM_{2.5}$  pollution was increased when the indoor air temperature was higher than outdoors, and the effect was worsened with the increasing NPL height. Thus, the conclusion can be drawn that the IAQ was inversely proportional to the NPL if the air temperature was higher indoors, while it was in direct proportion to NPL in summer. Considering the extent of occupants suffering from  $PM_{2.5}$  pollution, the NPL should be maintained at a lower position if the air temperature is higher indoors, whereas a higher position for the NPL is suggested in summer.

*The combined effect of air infiltration rate and filter on the indoor particle level.* The outdoor  $PM_{2.5}$  concentration in Suzhou ranged between 0 and 300  $\mu\text{g}/\text{m}^3$ . Furthermore, due to the technological developments in construction and production, buildings that have been built in recent years are generally more airtight than before.<sup>65,66</sup> Therefore, four different air infiltration rates, 0 ACH, 0.05 ACH, 0.1 ACH and 0.3 ACH, were selected to represent the well-insulated case, airtight case, typical case and leaky case, respectively.

From the simulation results, shown in Figure 9, occupants' health in a high-rise mechanically ventilated building is a deep concern since the indoor particulate pollution when the outdoor air quality has deteriorated. A suggestion for improving the IAQ in buildings is to install a high-efficiency air filter.<sup>67,68</sup> Hence, four air filters with different efficiencies were considered in the simulation. In this study, the filters used had Minimum Efficiency Reporting Value (MERV) 8, MERV 10, MERV 14 and MERV 16. According to the literature review,<sup>14,46</sup> the efficiency of removing  $PM_{2.5}$  with these four filters is 32.3%, 35.4%, 78% and 95%, respectively. Figure 12 displays the indoor particle levels' contour plots, which varied with outdoor air quality and air infiltration rate. In the plots, each graph's red curve represents the limit value of indoor particle concentration, 35  $\mu\text{g}/\text{m}^3$ , given in the WHO guideline.<sup>29</sup> According to WHO guidelines, the dangerous area above this curve highlights the indoor  $PM_{2.5}$  level that is too high for human health. Figure 12 shows that the indoor air quality was improved along with the use of higher filter efficiency, which is coincident with results reported in Ruan and Rim's work.<sup>10</sup> Furthermore, the results indicate that the indoor  $PM_{2.5}$  concentration can exceed the limit value even in a low infiltration rate if the outdoor air is highly polluted. Using higher MERV rating filters from

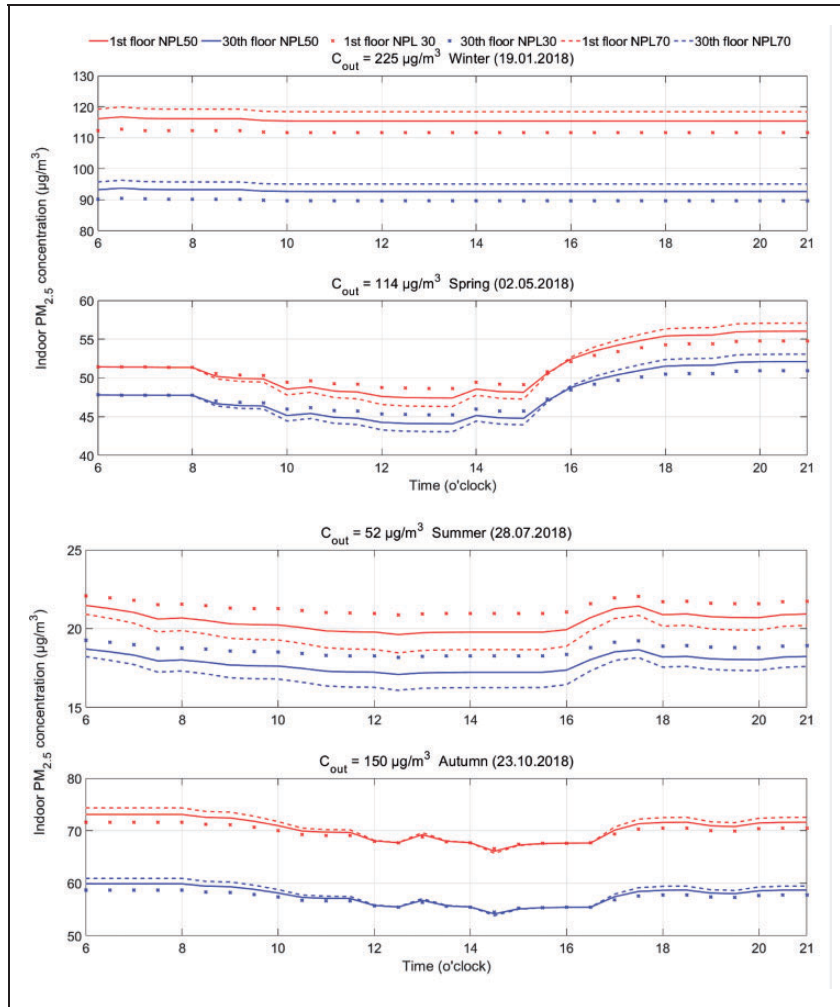


**Figure 11.** The variation law of indoor PM<sub>2.5</sub> concentration on each floor if the location of NPL changes.

MERV 10 to 16 can maintain indoor particle concentration within a healthy range for wider ranges of outdoor air conditions. However, the MERV 10 and MERV 14 are not effective enough to control IAQ in buildings if the building is leaky or the outdoor air is highly contaminated. For comparison, when the MERV 16 air filter was utilized in the ventilation system, the IAQ in the building would be in an acceptable range if the outdoor particle level was lower than 200 µg/m<sup>3</sup> or the air infiltration rate was lower than around 0.16 ACH. In addition, in some highly polluted cases, one filter system is not enough in Suzhou urban area, and a double-filter system should be considered.<sup>10</sup> Overall, the filters with a higher MERV rating have a better performance for maintaining IAQ in the building.

*The numerical model of the indoor PM<sub>2.5</sub> concentration at a steady state.* Figure 13 shows that the indoor PM<sub>2.5</sub> concentration varied with the air infiltration rate, the filter efficiency and the outdoor

concentration. Figure 13 presents that both the impact of the filter efficiency and the air infiltration rate on indoor particle levels are non-linear. If the infiltration rate was increased steadily and equally, the amplification of indoor particle concentrations would be increased if the air filter efficiency was increased. Meanwhile, the proportional reduction of the indoor PM<sub>2.5</sub> concentration was decreased with the increasing of the air infiltration rate when the filter efficiency was enhanced. This result reveals that the air infiltration rate can significantly affect the air filter's efficiency.<sup>22,45,64</sup> Furthermore, the steady-state indoor PM<sub>2.5</sub> level can be described by equation (12), which was derived by the curve fitting method. The relative fitting equation is shown below; note that the corresponding coefficient of determination is R<sup>2</sup> = 1

$$PM_{2.5} = (-8.9 \times 10^{-21})C_{out}^3 - (5.1 \times 10^{-18})C_{out}^2\lambda_i - (6.6 \times 10^{-18})C_{out}^2\beta + (1.0 \times 10^{-17})C_{out}^2$$

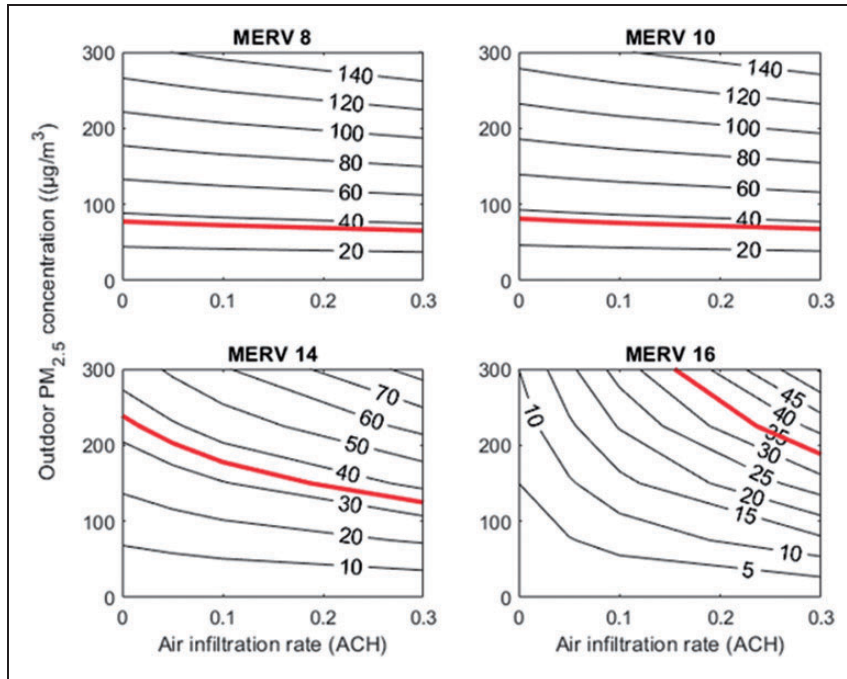


**Figure 12.** Combined effects of air infiltration rate and filters on the indoor PM<sub>2.5</sub> concentration under outdoor concentration from 0 to 300 µg/m<sup>3</sup>.

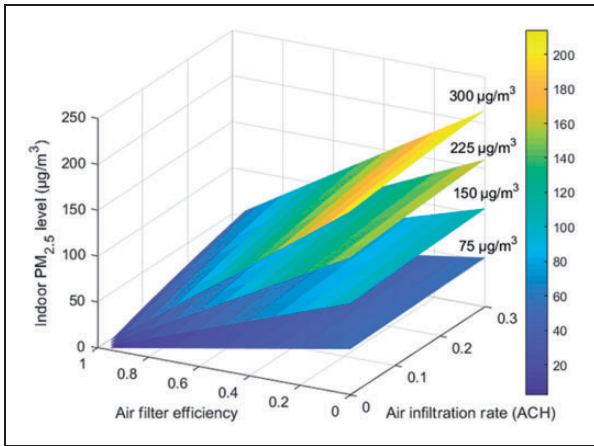


**Figure 13.** The increasing proportion of indoor PM<sub>2.5</sub> levels varied with the air infiltration rate and the filter efficiency. (The four surfaces from bottom to top represented the value range of the indoor PM<sub>2.5</sub> concentration under various air filter efficiency and air infiltration rate when outdoor PM<sub>2.5</sub> concentration was 75 µg/m<sup>3</sup>, 150 µg/m<sup>3</sup>, 225 µg/m<sup>3</sup>, 300 µg/m<sup>3</sup>, respectively.)

$$\begin{aligned}
 & -0.21C_{out}\lambda_i^2 + 0.37C_{out}\lambda_i\beta + 0.22C_{out}\lambda_i \\
 & + (1.2 \times 10^{-15})C_{out}\beta^3 - 0.66\beta + 0.67C_{out} + 23.5\lambda_i^3 \\
 & - 42.1\lambda_i^2\beta + 10.3\lambda_i^2 + (1.0 \times 10^{-12})\lambda_i\beta^2 + 12.6\lambda_i\beta \\
 & - 5.1\lambda_i + (6.4 \times 10^{-15})\beta^3 - (3.5 \times 10^{-13})\beta^2 - 0.53\beta \\
 & + 0.24314
 \end{aligned}$$

(12)

where PM<sub>2.5</sub> is the indoor PM<sub>2.5</sub> concentration at the steady-state level in µg/m<sup>3</sup>, C<sub>out</sub> is the outdoor particle level in µg/m<sup>3</sup> and λ<sub>i</sub> is the air infiltration rate in ACH, and β is the air filter efficiency. Moreover, the simulation results show that the steady state of the indoor particle concentration was correlated with the particle deposition rate when the building is well-insulated, and there is no air filter installed.<sup>69,70</sup> The particle deposition mechanism is affected by many factors, including particle characteristics, room air velocity, room surface characteristics<sup>71</sup> and also air filter efficiency.<sup>50</sup> Thatcher et al.<sup>71</sup> reported that the particles' deposition rate lower than about 2.5 µm would range typically between 0.1 h<sup>-1</sup> and 1.0 h<sup>-1</sup>.

In addition, the model was verified by findings from several previous studies. Ruan and Rim<sup>10</sup> simulated the indoor PM<sub>2.5</sub> level with three different air filters in Beijing. The three selected filter efficiencies for removing PM<sub>2.5</sub> were 30%, 65% and 95% in their studies. The input data were 1.043 ACH, 0.028 ACH, 0.5 h<sup>-1</sup> as the outdoor air ventilation rate, infiltration rate and deposition rate, respectively. Substituting these values into equation (12) yields slightly higher indoor PM<sub>2.5</sub> concentrations than the published results. Moreover, Ben-David and Waring<sup>72</sup> investigated the indoor to outdoor ratios of six air pollutants under four ventilation cases in 14 USA cities, considering the factors, including air exchange rate, infiltration rate, meteorological conditions and filter efficiency. When inputting

their data into equation (12), the obtained indoor  $PM_{2.5}$  concentrations were also slightly higher than the reported results. This is because the recirculation process on the ventilation system was not considered in this study. Meanwhile, the fresh air supply rate was slightly higher in their study.

Therefore, the output of equation (12) is coincident with the results reported by these published researches. As a result, this equation can be applied to other buildings, and designers could use this numerical model to determine suitable air filter efficiency and acceptable air infiltration rate based on outdoor air conditions.

## Conclusion

This study investigated the impact of outdoor air pollutants on IAQ in a high-rise office building. As a case study, this paper analysed the impact of atmospheric weather conditions on air infiltration in Suzhou. It employed existing strategies using measured data, collected data and numerical simulation to assess the impact of outdoor air pollutants on IAQ in a high-rise office building. The IAQ in a high-rise building was analysed considering the stack effect, wind effect, infiltration rate, outdoor air pollution rate, seasonal change, air filter efficiency and floor height, which had significantly impacted on the IAQ.

Based on the analysis, the temperature difference between indoor and outdoor and the outdoor wind speed was proportional to the pressure difference between indoor and outdoor, while the pressure difference between wind and south facades was proportional to the wind angle with a negative gradient. As a result of the seasonal effects on the IAQ found on each floor of the building, the IAQ was worst in winter, followed by spring, autumn and summer. Numerical simulation showed that the IAQ differed from floor to floor in the high-rise building. The results indicate that the indoor particle concentration was lower on higher floors than on the lower floors in a high-rise building. According to the simulation results, the air filter efficiency was negatively related to the indoor particle concentration. Hence, to control the indoor PM level within the limit value, a filter with at least a high-efficiency air filter is required, and a double-filter system should be used if the outdoor air is highly polluted. In addition, a numerical model of the reduction proportion of indoor  $PM_{2.5}$  level at steady state was developed to help designers determine the suitable air filter efficiency and acceptable air infiltration rate based on outdoor air conditions.

Due to the limitations of the experiment site to measure the actual infiltration rate in a high-rise building, the on-site measurement of infiltration rate was not conducted to validate the numerical simulation results.

This limitation may make the validation of the numerical simulation result difficult. However, the results were numerically calculated following the ASHRAE procedure. Hence, future study is needed for validating the findings of this study. Moreover, outdoor air pollutants' vertical profiles around the building facade could vary with the building's surrounding environment, outdoor emission sources and meteorological conditions. Future studies are scheduled to investigate outdoor air pollutants' vertical profiles depending on the multiple factors discussed earlier.

## Authors' contribution

All authors contributed equally to the preparation of this article.

## Authors' Note

Moon Keun Kim is now affiliated with Department of Civil Engineering and Energy Technology, Oslo Metropolitan University.



## Declaration of conflicting interests

The author(s) declared no potential conflicts of interest with respect to the research, authorship, and/or publication of this article.

## Funding

The author(s) disclosed receipt of the following financial support for the research, authorship, and/or publication of this article: This work was supported by the Research Development Fund (RDF 15-02-32) of Xi'an Jiaotong – Liverpool University, Zhejiang Provincial Natural Science Foundation (LY19E080001), the UK ICE Research Development Enabling Fund (ICE\_RDF\_2020), and the Department of Civil Engineering and Energy Technology of Oslo Metropolitan University.

## ORCID iDs

Moon Keun Kim  <https://orcid.org/0000-0001-9614-5412>  
Bing Chen  <https://orcid.org/0000-0003-2273-4104>

## References

1. Yang M, Chu C, Bloom MS, Li S, Chen G, Heinrich J, Markevych L, Knibbs LD, Bowatte G, Dharmage SC, Komppula M, Leskinen A, Hirvonen MR, Roponen M, Jalava P, Wang SQ, Lin S, Zeng XW, Hu LW, Liu KK, Yang BY, Chen W, Guo Y and Dong GU. Is smaller worse? New insights about associations of  $PM_{10}$  and respiratory health in children and adolescents. *Environ Int.* 2018; 120: 516–524.
2. Wang H. Study shows  $PM_{10}$  air pollution is most harmful, [http://usa.chinadaily.com.cn/china/2013-10/28/content\\_17061997.htm](http://usa.chinadaily.com.cn/china/2013-10/28/content_17061997.htm) (2013, accessed 19 July 2019).
3. Mehta S, Shin H, Burnett R, North T and Cohen AJ. Ambient particulate air pollution and acute lower respiratory infections: a systematic review and implications

- for estimating the global burden of disease. *Air Qual Atmos Health* 2013; 6: 69–83.
4. Wallace LA. *Total Exposure Assessment Methodology (team) Study Summary and Analysis, Volume I Final Report*. Report No. PB-88-100060/XAB; EPA-600/6-87/002A United States NTIS. Environmental Protection Agency, Washington, DC (USA): Office of Acid Deposition, Environmental Monitoring, and Quality Assurance, 1987.
  5. Liu Y, Chen R, Shen X and Mao X. Wintertime indoor air levels of PM<sub>10</sub>, PM<sub>2.5</sub> and PM<sub>1</sub> at public places and their contributions to TSP. *Environ Int* 2004; 30: 189–197.
  6. CTBUH. *Tall buildings in numbers: 2017 year in review*. Chicago, IL: Council on Tall Buildings and Urban Habitat, 2017.
  7. Miller SL, Facciola NA, Toohey D and Zhai J. Ultrafine and Fine particulate matter inside and outside of mechanically ventilated buildings. *Int J Environ Res Public Health* 2017; 14: 128.
  8. Scibor M. Are we safe inside? Indoor air quality in relation to outdoor concentration of PM<sub>10</sub> and PM<sub>2.5</sub> and to characteristics of homes. *Sustain Cities Soc* 2019; 48: 101537.
  9. Morawska L, Ayoko GA, Bae GN, Buonanno G, Chao CYH, Clifford S, Fu SC, Hanninen O, He C, Isaxon C, Mazaheri M, Salthammer T, Waring MS and Wierzbicka A. Airborne particles in indoor environment of homes, schools, offices and aged care facilities: the main routes of exposure. *Environ Int* 2017; 108: 75–83.
  10. Ruan T and Rim D. Indoor air pollution in office buildings in mega-cities: effects of filtration efficiency and outdoor air ventilation rates. *Sustain Cities Soc* 2019; 49: 101609.
  11. Moschandreas J, Yoon SH and Demirev D. Validation of the indoor environmental quality conceptual model. *Build Res Inf* 2006; 34: 483–495.
  12. Cao SJ, Yu CW and Luo XL. New and emerging building ventilation technologies. *Indoor Built Environ* 2020; 29: 483–484.
  13. Kim MK and Choi JH. Can increased outdoor CO<sub>2</sub> concentrations impact on the ventilation and energy in buildings? A case study in Shanghai, China. *Atmos Environ* 2019; 210: 220–230.
  14. Stephens B. Evaluating the sensitivity of the mass-based particle removal calculations for HVAC filters in ISO 16890 to assumptions for aerosol distributions. *Atmosphere* 2018; 9: 85.
  15. Azimi P, Zhao D and Stephens B. Estimates of HVAC filtration efficiency for fine and ultrafine particles of outdoor origin. *Atmos Environ* 2014; 98: 337–346.
  16. Brown C and Gorgolewski M. Understanding the role of inhabitants in innovative mechanical ventilation strategies. *Build Res Inf* 2015; 43: 210–221.
  17. Feng ZB, Yu CW and Cao SJ. Fast prediction for indoor environment: models assessment. *Indoor Built Environ* 2019; 28: 727–730.
  18. Deng GF, Li ZH, Wang ZC, Gao J, Xu Z, Li J and Wang Z. Indoor/outdoor relationship of PM<sub>2.5</sub> concentration in typical buildings with and without air cleaning in Beijing. *Indoor Built Environ* 2017; 26: 60–68.
  19. Kim MK and Baldini L. Energy analysis of a decentralized ventilation system compared with centralized ventilation systems in European climates: based on review of analyses. *Energy Build* 2016; 111: 424–433.
  20. Meggers F, Pantelic J, Baldini L and Kim MK. Evaluating and adapting low exergy systems with decentralized ventilation for tropical climates. *Energy Build* 2013; 67: 559–567.
  21. Goubran S, Qi D, Saleh WF and Wang L. Comparing methods of modeling air infiltration through building entrances and their impact on building energy simulations. *Energy Build* 2017; 138: 579–590.
  22. Prignon M and Van Moeseke G. Factors influencing airtightness and airtightness predictive models: a literature review. *Energy Buildings* 2017; 146: 87–97.
  23. Malmqvist T. Environmental rating methods: selecting indoor environmental quality (IEQ) aspects and indicators. *Build Res Inf* 2008; 36: 466–485.
  24. ASHRAE I. *2017 ASHRAE handbook: fundamentals*. SI edition. Atlanta: The American Society of Heating, Refrigerating and Air Conditioning Engineers, 2017.
  25. Jones BM, Lowe RJ, Davies M, Chalabi Z and Ridley I. Modelling uniformly porous facades to predict dwelling infiltration rates. *Build Serv Eng Res Technol* 2013; 35: 408–416.
  26. Liu D-L and Nazaroff WW. Particle penetration through building cracks. *Aerosol Sci Technol* 2003; 37: 565–573.
  27. Li A, Ren T, Yang C, Lv W and Zhang F. Study on particle penetration through straight, L, Z and wedge-shaped cracks in buildings. *Build Environ* 2017; 114: 333–343.
  28. Liu G, Xiao M, Zhang X, Gal C, Chen X, Liu L, Pan S, Wu J, Tang L and Clements-Croome D. A review of air filtration technologies for sustainable and healthy building ventilation. *Sustain Cities Soc* 2017; 32: 375–396.
  29. WHO. *Air quality guidelines global update 2005: particulate matter, ozone, nitrogen dioxide and sulfur dioxide*. Copenhagen: World Health Organization, Regional Office for Europe, 2006.
  30. Diebel J, Norda J and Kretschmer O. *Average weather in Suzhou*, <https://weatherspark.com/y/135845/Average-Weather-in-Suzhou-China-Year-Round> (2019, accessed 28 September 2019).
  31. ASHRAE Standard 62.1-2010. *Ventilation for acceptable indoor air quality*. Atlanta: The American Society of Heating, Refrigerating and Air Conditioning Engineers, 2010.
  32. Wu Y, Hao JM, Fu LX, Wang Z and Tang U. Vertical and horizontal profiles of airborne particulate matter near major roads in Macao, China. *Atmos Environ* 2002; 36: 4907–4918.
  33. Liu F, Zheng XH and Qian H. Comparison of particle concentration vertical profiles between downtown and urban forest park in Nanjing (China). *Atmos Pollut Res* 2018; 9: 829–839.



34. Wang J. Suzhou daily average outdoor dry-bulb air temperature from 1st of January 2018 to 31st of December 2018 [www.aqstudy.cn/](http://www.aqstudy.cn/) (2019, accessed 21 September 2019).
35. Huiji Data. *Suzhou daily average wind speed from 1st of January 2018 to 31st of December 2018*. <http://hz.zc12369.com/> (2019, accessed 28 September 2019).
36. Tom B. *Temperature and altitude*, [http://grc.nasa.gov/www/k-12/problems/Jim\\_Naus/TEMPandALTITUDE\\_ans.htm](http://grc.nasa.gov/www/k-12/problems/Jim_Naus/TEMPandALTITUDE_ans.htm) (2014, accessed 8 October 2019).
37. ASHRAE Standard 55-2010. *Thermal environmental conditions for human occupancy*. Atlanta: The American Society of Heating, Refrigerating and Air Conditioning Engineers, 2010.
38. Huang W, Xie X, Qi X, Huang J and Li F. Determination of particle penetration coefficient, particle deposition rate and air infiltration rate in classrooms based on monitored indoor and outdoor concentration levels of particle and carbon dioxide. *Proc Eng* 2017; 205: 3123–3129.
39. Diapouli E, Chaloulakou A and Koutrakis P. Estimating the concentration of indoor particles of outdoor origin: a review. *J Air Waste Manag Assoc* 2013; 63: 1113–1129.
40. Quang TN, He C, Morawska L and Knibbs LD. Influence of ventilation and filtration on indoor particle concentrations in urban office buildings. *Atmos Environ* 2013; 79: 41–52.
41. Yu CKH, Li M, Chan V and Lai ACK. Influence of mechanical ventilation system on indoor carbon dioxide and particulate matter concentration. *Build Environ* 2014; 76: 73–80.
42. EPA. Indoor particulate matter \_ indoor air quality (IAQ), [www.epa.gov/indoor-air-quality-iaq/indoor-particulate-matter](http://www.epa.gov/indoor-air-quality-iaq/indoor-particulate-matter) (2019, accessed 21 September 2019).
43. Liu DL and Nazaroff WW. Modeling pollutant penetration across building envelopes. *Atmos Environ* 2001; 35: 4451–4462.
44. Shi Y and Li X. A study on variation laws of infiltration rate with mechanical ventilation rate in a room. *Build Environ* 2018; 143: 269–279.
45. Shi Y and Li X. Purifier or fresh air unit? A study on indoor particulate matter purification strategies for buildings with split air-conditioners. *Build Environ* 2018; 131: 1–11.
46. ASHRAE 52.2-1999. *Method of testing general ventilation air-cleaning devices for removal efficiency by particle size (ANSI approved)*. Atlanta: The American Society of Heating, Refrigerating and Air Conditioning Engineers, 1999.
47. Wang ZT, Liu C, Hua Q, Zheng X, Ji W and Zhang X. Effect of particulate iron on tracking indoor PM<sub>2.5</sub> of outdoor origin: a case study in Nanjing, China. *Indoor Built Environ* 2021; 30: 711–723.
48. Ng LC, Musser A and Persily Ak Emmerich SJ. *Airflow and indoor air quality b models of DOE reference commercial buildings*. NIST Pubs. Report no. 1734, Gaithersburg, MD, 2012.
49. Chen C, Zhao B, Zhou W, Jiang X and Tan Z. A methodology for predicting particle penetration factor through cracks of windows and doors for actual engineering application. *Build Environ* 2012; 47: 339–348.
50. Rackes A and Waring MS. Modeling impacts of dynamic ventilation strategies on indoor air quality of offices in six US cities. *Build Environ* 2013; 60: 243–253.
51. Kim MK, Barber C and Srebric J. Traffic noise level predictions for buildings with windows opened for natural ventilation in urban environments. *Sci Technol Built Environ* 2010; 23: 726–735.
52. Vornanen-Winqvist C, Toomla S, Ahmed K, Kurnitski J, Mikkola R and Salonen H. The effect of positive pressure on indoor air quality in a deeply renovated school building – a case study. *Energy Proc* 2017; 132: 165–170.
53. Price PN, Shehabi A, Chan RW and Gadgil AJ. *Indoor-outdoor air leakage of apartments and commercial buildings*. LBNL-60682. Berkeley: Lawrence Berkeley National Laboratory, 2006.
54. Li XL, Wang JS, Tu XD, Liu W and Huang Z. Vertical variations of particle number concentration and size distribution in a street canyon in Shanghai, China. *Sci Total Environ* 2007; 378: 306–316.
55. Kalaiarasan M, Balasubramanian R, Cheong KWD and Tham KW. Traffic-generated airborne particles in naturally ventilated multi-storey residential buildings of Singapore: vertical distribution and potential health risks. *Build Environ* 2009; 44: 1493–1500.
56. Zhang YF, Xu H, Tian YZ, Shi GL, Zeng F, Wu JH, Zhang XY, Li X, Zhu T and Feng YC. The study on vertical variability of PM<sub>10</sub> and the possible sources on a 220 m tower, in Tianjin, China. *Atmos Environ* 2011; 45: 6133–6140.
57. Deng XJ, Li F, Li YH, Huang H and Liu X. Vertical distribution characteristics of PM in the surface layer of Guangzhou. *Particuology* 2015; 20: 3–9.
58. Peng ZR, Wang DS, Wang ZY, Wang Z, Gao Y and Lu S. A study of vertical distribution patterns of PM<sub>2.5</sub> concentrations based on ambient monitoring with unmanned aerial vehicles: a case in Hangzhou, China. *Atmos Environ* 2015; 123: 357–369.
59. Azimi P, Zhao HR, Fazli T, Zhao D, Faramarzi A, Leung L and Stephens B. Pilot study of the vertical variations in outdoor pollutant concentrations and environmental conditions along the height of a tall building. *Build Environ* 2018; 138: 124–134.
60. Liu P, Zhao C, Zhang Q, Liu P, Deng Z, Huang M, Ma X and Tie X. Aircraft study of aerosol vertical distributions over Beijing and their optical properties. *Tellus B: Chem Phys Meteorol* 2009; 61: 756–767.
61. Xiao Z, Wu J, Han S, Zhang Y, Xu H, Zhang X, Shi G and Feng Y. Vertical characteristics and source identification of PM<sub>10</sub> in Tianjin. *J Environ Sci* 2012; 24: 112–115.
62. Li XB, Wang DS, Lu QC, Peng ZR and Wang ZY. Investigating vertical distribution patterns of lower tropospheric PM<sub>2.5</sub> using unmanned aerial vehicle measurements. *Atmos Environ* 2018; 173: 62–71.
63. Cheng X, Zhang H, Pan W, Liu S, Zhang M, Long Z, Zhang T and Chen Q. Field study of infiltration rate and

- its influence on indoor air quality in an apartment. *Proc Eng* 2017; 205: 3954–3961.
64. Younes C, Shdid CA and Bitsuamlak G. Air infiltration through building envelopes: a review. *J Build Physics* 2011; 35: 267–302.
65. Awbi HB. Ventilation for good indoor air quality and energy efficiency. *Energy Proc* 2017; 112: 277–286.
66. Spuru P and Simona PL. A review on interactions between energy performance of the buildings, outdoor air pollution and the indoor air quality. *Energy Proc* 2017; 128: 179–186.
67. Kim MK and Leibundgut H. Performance of novel ventilation strategy for capturing CO<sub>2</sub> with scheduled occupancy diversity and infiltration rate. *Build Environ* 2015; 89: 318–326.
68. Kim MK, Baldini L, Leibundgut H, Wurzbacher J and Piatkowski N. A novel ventilation strategy with CO<sub>2</sub> capture device and energy saving in buildings. *Energy Build* 2015; 87: 134–141.
69. Howard-Reed C, Emmerich SJ and Wallace L. *Deposition rates of fine and coarse particles in residential buildings: Literature review and measurements in an occupied townhouse*. NISTIR 7068, Gaithersburg, MD: National Institute of Standards and Technology, 2003.
70. Ben-David T, Wang S, Rackes A and Waring MS. Measuring the efficacy of HVAC particle filtration over a range of ventilation rates in an office building. *Build Environ* 2018; 144: 648–656.
71. Thatcher TL, Lai ACK, Moreno-Jackson R, Sextro RG and Nazaroff WW. Effects of room furnishings and air speed on particle deposition rates indoors. *Atmos Environ* 2002; 36: 1811–1819.
72. Ben-David T and Waring MS. Impact of natural versus mechanical ventilation on simulated indoor air quality and energy consumption in offices in fourteen U.S. cities. *Build Environ* 2016; 104: 320–336.